

Optical Interference Reduction with Spatial Filtering Receiver for Vehicular Visible Light Communication

Claas Tebruegge^{1,2}, Qiaoshuang Zhang³ and Falko Dressler¹

Abstract— We present a novel receiver-based interference reduction mechanism for Vehicular Visible Light Communication (V-VLC). V-VLC, in combination with Radio Frequency (RF)-communication, is a technology that is promising to enable a reliable communication link for a number of Intelligent Transportation Systems (ITS) applications such as cooperative driving. Both technologies complement each other to overcome technology-dependent limitations. Particularly, V-VLC is drawing attention as it is able to provide rather high capacity links. Nevertheless, it was observed that V-VLC suffers from interference caused by ambient light as well as modulated light sources, for instance LED signage. To overcome this barrier, we propose a system that makes use of the Line of Sight (LOS)-characteristic and imaging optics. More precisely, we are using a spatial light modulator in the form of a Liquid Crystal (LC)-panel to spatially filter interference and ambient light, thereby reducing interference to a minimum. We built and tested a photodiode-based receiver for V-VLC and, validated by simulations and measurements, we demonstrate the capability of the system.

I. INTRODUCTION

Since the invention of the car, the number of cars increases rapidly. Especially in Asia, this trend has accelerated even faster in the last decade. With increasing number of cars, more advanced methods are needed to make traffic safer and more efficient. In combination with automated driving, connected driving and Intelligent Transportation Systems (ITS) are promising technologies to be the next big step [1]. Vehicles can share their perception and react cooperatively, which lowers the risk of accidents dramatically and increases efficiency in terms of fuel consumption, time and street utilization. Some modern vehicles are already equipped with Radio Frequency (RF)-based communication devices. For a certain range of penetration rate this offers benefits in comfort, safety, and efficiency. Available (and standardized) technologies include Dedicated Short Range Communication (DSRC) (including the European ETSI ITS-G5 [2] and the U.S. IEEE WAVE standards [3]) and Cellular V2X (C-V2X) [4]. However, DSRC-based communication suffers from multiuser interferences and limited bandwidth. Besides, C-V2X is only particularly beneficial if there is a perfect cellular coverage [5]. To overcome these limitations, Visible Light Communication (VLC) stands out as a promising candidate due to the propagation of light and the associated scalability, the license free spectrum and dual use of vehicles' LEDs [6]. The capability of Vehicular Visible Light Communication

(V-VLC) has especially been shown in helping with the communication on rather short distances such as in platooning applications [7]–[9], and frequently also in forming a heterogeneous networking approach in combination with RF-based solutions [10], [11]. Nevertheless, studies have shown that V-VLC has to struggle with low signal strength at large distances and interference of modulated light sources [12]. A powerful solution to deal with these problems is an advanced optical receiver. In this paper, we present an advanced Liquid Crystal based Optical Receiver (LC-Rx), which is able to adapt the Field of View (FoV) of the receiver and filter out interference spatially. In this way, it is able to optically reduce interference for V-VLC systems.

Our main contributions can be summarized as follows:

- We present a novel programmable optical filter system to spatially filter interference at a VLC receiver (Section III);
- we detail the optical design with a focus on vehicular applications (Section IV); and
- we thoroughly investigate the consequential performance improvements of the overall V-VLC system (Section V).

II. RELATED WORK

In VLC, the optical signal is perceived by an optical receiver at the frontend, followed by demodulation and decoding processing. Commonly, two types of optical receivers are used in VLC: either an image sensor or a photodiode. A major advantage of using an image sensor is a broader communication range enabled by its large FoV. Besides, in V-VLC, all the light sources within the FoV of the receiver will form images on the image sensor, allowing one to spatially filter out the interference and at the same time making it possible for processing light from multiple signal sources independently. However, the communication data rates are severely constrained by camera's low frame rate. Most of the low-cost cameras have only 15-30 frames per second (fps) [13]. The fps rate of commonly used ones in smartphones are no more than 40 [14]. Therefore, the low bandwidth and low data rates are the obstacles the image sensor has to come across before efficiently being applied in a VLC system. High-speed cameras can be used to address the issue, with the data rates per pixel rising up to 54 Mbit/s [15], but this comes along with high complexity and high costs, which again pose a hurdle for mass production in automotive application.

An alternative is the photodiode, whose high bandwidth enables Gbit/s data rates [16] and comes at a lower cost than an image sensor. However, in contrast to the image sensor, a photodiode integrates all the light incident on its

¹ Dept. of Computer Science, Paderborn University, Germany

² HELLA GmbH & Co. KGaA, Lippstadt, Germany

³ Light Technology Institute, Karlsruhe Institute of Technology, Germany
{tebruegge,dressler}@ecs-labs.org;qiaoshuang.zhang@kit.edu

active area and, thus, cannot process interference in a spatial manner. Hence, relatively, more ambient light is received by the photodiode, which results in the increased shot noise and other noises generated by interference. Another drawback is its limited dynamic range, which makes it prone to saturation in case of a high input power, e.g., when the sun is at the horizon level or when the light sources emit intensively. The noises can be reduced by decreasing the FoV of the receiver. However, this consequently narrows down the lateral communication range. Therefore, a trade-off between Signal-to-Noise Ratio (SNR) and the communication range has to be made. A photodiode is usually followed by a preamplifier which amplifies the electrical signal by a certain gain. In the following context the combination of both is called Photodetector (PD). As a consequence, an optimal gain is also critical and should be chosen to realize long-distance or weak-signal communication without saturating the PD. A fully featured photodiode-based V-VLC system has been presented just recently in [17].

With an aim to mitigate interference in free-space optical communications, angle-diversity receivers consisting of an array of receivers are applied in infrared [18], ultraviolet [19], and visible light communication [20]. Similarly, by exploiting the spatial characteristics of light sources in VLC, a dynamic vision sensor has been proposed to only report significant changes in the illumination of each pixel, thereby increasing the throughput of the system [21]. Nevertheless, these methods confront with issues such as the trade-off between high system complexity and complicated algorithms.

The idea of combining optical spatial filtering and a single detector was first brought up by [22], where a Digital Micromirror Device (DMD) is used as the component for filtering. By controlling the tilting angle of each micromirror, light rays coming from the objects of interest are reflected and oriented towards the detector, while other rays are reflected into an absorber. By this means, the noise level is to a great extent lowered without any costs of the bandwidth. However, some drawbacks come with the DMD: first, the folding of the optical path may reduce the size in one dimension, but increase it in the other direction, which makes it less compact for implantation; second, a DMD only allows a highly limited angle of incidence, which increases the requirements on the optics and thus increases the complexity of the system; last but not least, a Liquid Crystal (LC) panel can be easily controlled by even a simple microcontroller, while currently commercially available DMDs requires additional controlling boards.

Compared to a DMD that performs filtering in a reflective way, a LC panel with the ability of transmissive filtering seems to be a promising competitor. With a LC panel, all of our components are centered with respect to a common optical axis, which eases the burden of alignment. Besides, in a DMD, each micromirror performs like a pixel in a fully white or fully black state, while with LC pixels, it is possible to have grayscales in between and, thus, more states of a single pixel can be chosen. To our knowledge a LC panel is applied in a VLC receiver's prototype for the first time,

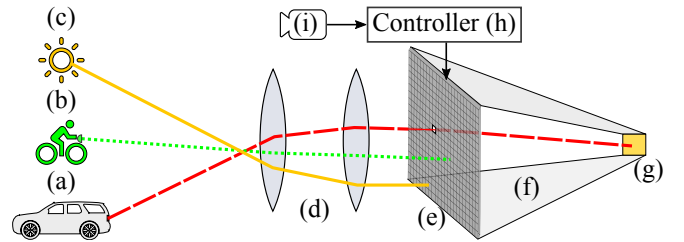


Fig. 1. Schematic layout of the receiver

combined with a PD. Simulation and empirical evaluations are also completed based on this prototype and are introduced in the following sections.

III. SYSTEM DESIGN

The conceptual layout of the receiver is illustrated in Figure 1. The signal transmitter is a lamp of a car (a); a cyclist is riding next to the car and the lamp of the bike (b) represents one of the interference sources; in daylight conditions, when the sun (c) is within the FoV of the receiver, it is a considerable noise source which may blind the receiver. All the light from these sources is collected by the front optics (d). After mapping, the images of the light sources are separated spatially at the focal plane where a LC panel (e) is placed. By controlling the state of the pixels, those within region where the image of (a) is located are switched to "on" state and the others are at "off" state. Thereby, the light forming the image of (a) is allowed to penetrate the panel and be guided by the light guiding tube (f) to the PD (g), whilst the light emitted from (b) and (c) is blocked by the panel. The PD is linked to the controller (h) of the LC panel. The controller receives information about the position of communication partners from an aiding camera (i). When the transmitter is at a short distance to the receiver, the signal may become so strong that the PD gets saturated, then the controller is able to decrease the number of pixels which are at "on" state or alter the transmittance of the pixels in an almost continuous way to reduce the signal intensity, so that the PD can always work in its optimum operation range, ensuring the detection process goes on smoothly.

IV. OPTICAL DESIGN

Before the design of the front optical system, the application scope of the receiver has to be defined. In terms of longitudinal communication range, the minimum distance which should be kept by two vehicles driving along a highway in Germany is considered. The safety distance one should keep to the forward vehicle in m equals half of the numerical value of driving speed in km/h, according to a rule of thumb. Taking the speed of 100 km/h into consideration, the safety distance is then 50 m. Therefore, within 50 m there lies the necessity to establish communication between two cars. As for the lateral communication range, an overtaking scenario should be taken into consideration. A large FoV of 100° is sufficient for the general applications: the width of one lane is typically about 3 m according to German Road Traffic

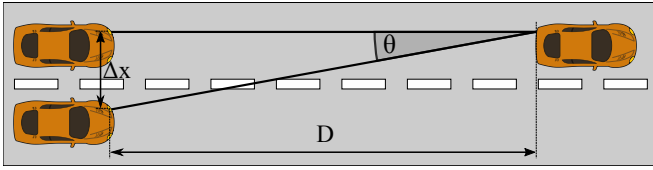


Fig. 2. Example scenario where one signal source and one interference source are present in a vehicular VLC application

Regulations¹ and the width of the car is about 2 m. With such a FoV, communication can cover both neighboring lanes from $D = 3$ m longitudinally away from the receiver, as shown in Figure 2. Therefore, assuming a car on the left lane just overtakes a car on the right lane, with a lateral distance of $\Delta x = 0.5$ m between the transmitter and receiver, after a longitudinal distance smaller than 0.5 m the car on the right is able to tell the left car if it is safe for it to merge onto the right lane, thus increasing driving safety.

The front optics is designed with ZEMAX and is supposed to realize three functions. First, a basic mapping function is expected. However, it is not necessary to minimize aberrations like distortion and astigmatism in mapping, only the sizes of the image spots are important for the control of the LC panel. Second, the front optics is supposed to extend the active area of the receiver, which means a large effective pupil size of the optical system is desired. With the receiving area increased, not only more signal light can be collected, but also the SNR can increase. Third, in order to have a broad lateral communication range and reduce the probability of losing the connection, a wide FoV of 100° is essential. However, the main difficulty is to fulfill these requirements while using as few optical elements as possible, in order to decrease the loss of signal. Besides, fewer elements are desirable considering cost-saving in the automotive industry.

The optical design was initiated with two elements. The initial structure of the first lens was chosen to be a bi-convex type, considering the refractive power of the system, also a bi-convex lens is less subject to spherical aberrations. Because the spot size is an important criterion in optical design and chromatic aberration is one of the causes of large spot sizes, the second element was set to be a doublet lens which is able to reduce chromatic aberrations and paraxial spherical

¹Original in German: Richtlinien für die Anlage von Straßen

TABLE I
SPECIFICATIONS OF THE LC PANEL

Parameter	Value
Type	Monochrome
Display size	2.2-inch diagonal
Technology	α -Silicon, VA
Resolution	320×240
Pixel size	$141 \mu\text{m} \times 141 \mu\text{m}$
Transmittance	$\sim 20\%$
Contrast ratio	~ 3400
Operating temperature	-20°C to 70°C

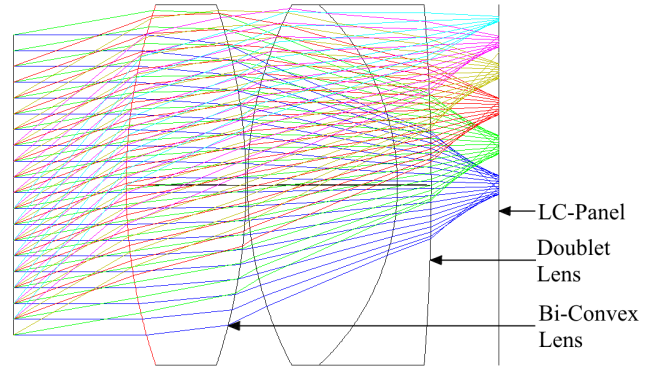


Fig. 3. Layout of the optical design in xz-plane

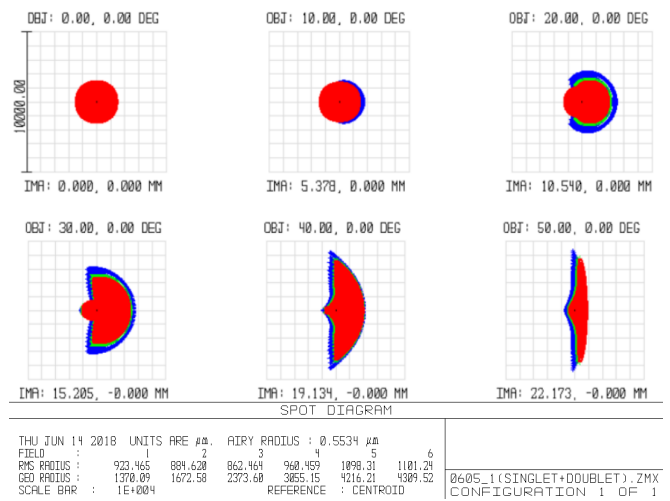


Fig. 4. Spot diagram of the optics for each field angle.

aberrations. The doublet lens has to be positive as well to ensure the refractive power of the whole system. A LC panel is put at the image plane with specifications listed in Table I.

After the optimization, the elements are substituted by off-the-shelf lenses, and the two-dimensional layout of the optical system can be seen in Figure 3. The figure is given in xz-plane (top view) with rays colored by semi-fields from 0° to 50° with an interval of 10° . The vertical and lateral FoV of the system is 60° and 100° , respectively. The entrance pupil dimension is 40 mm in diameter, which leads to a received signal power of up to four times larger than the one received using only the PD with an active area of 100 mm^2 .

A helpful tool to evaluate the optical system is the spot diagram, as given in Figure 4. It can be seen that with the field angle increasing, due to off-axis aberrations, the radius of the spot slightly decreases in the lateral direction but stretches vertically. The influence of this effect on the receiver's performance is rather small in typical traffic scenarios. Strong noise sources like billboards or traffic lights are typically located with either an enough distance or a large incident angle to the signal source. Therefore, the images from the sources can be separated even with a stretched spot. High requirements for the spot size are usually important for the

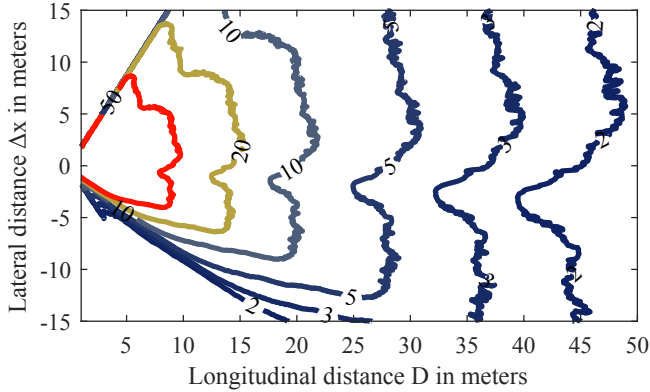


Fig. 5. Isolux pattern of the high beam in Lux

area around the optical center, because more signal and noise sources are imaged in this area under common traffic scenarios and are expected to be close to each other. By controlling the LC panel the effects of interference can be minimized or avoided.

Another advantage of such a front optics comes from the type of mapping. Since most common lenses follow the $f - \tan\theta$ mapping where f is the focal length and θ is the field angle, the incremental distance on the image plane corresponds to the incremental distance on the object plane [23]. But for large-FoV lenses, the mapping does not follow $f - \tan\theta$ anymore, but approximates the mapping where the incremental distance on the image plane corresponds to the incremental angle in the object space. This kind of mapping is beneficial for V-VLC applications since in most cases the signal light comes from the near-axis region and the resolution for near-axis region should be reasonably higher than for far off-axis regions.

V. EVALUATION

With the designed optics, the behavior of the whole receiver is simulated in MATLAB. The signal source is a left high beam and its illumination pattern is shown in Figure 5. The PD is a silicon detector PDA 100 from Thorlabs, with an active area of $10 \text{ mm} \times 10 \text{ mm}$ and a response range covering the visible light spectrum. A pre-amplifier is integrated in the PD which converts and amplifies the received photocurrent into voltage. After the LC panel, the residual light has to reach the small active area of the PD for detection. During this process, no imaging or mapping of the light is needed; therefore, for ease of practical application, a light guiding tube in a pyramidal horn shape is adopted, which is formed by four flat mirrors. Because of the slope of the tube there exist back reflections, which can be recycled by depositing a transfective film on the back side of the LC panel. In simulations a perfect recycling of the light after LC panel filtering is presumed.

The simulation is carried out under two scenarios. The first one is in an outdoor environment with brightest sunlight, where the illuminance is assumed to be 100 klx and is homogeneously distributed in the space. One signal source (a

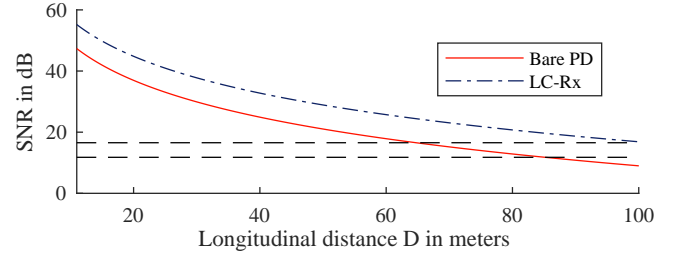


Fig. 6. SNR at the receiver

left high beam) is present in front of the receiver. The SNR can now be calculated as

$$SNR = \frac{I_{signal}^2}{\sigma_{shot}^2 + \sigma_{thermal}^2}, \quad (1)$$

where I_{signal} is the photocurrent induced by the signal power and σ_{shot} and $\sigma_{thermal}$ are the variances of the shot noise and thermal noise, respectively.

A Bit Error Rate (BER) of less than 10^{-6} is required in a communication channel to establish a reliable link. This corresponds to 16.55 dB and 11.78 dB with On-Off Keying (OOK) and 8-PPM schemes using the formulas given in [24], taking into account the usable average signal power. When only one PD with neither optics nor LC panel is used as the receiver, the SNR of the system varies with the relative positions between the transmitter and the receiver, indicated by the blue curve in Figure 6.

From the figure we can see that when the simplest OOK scheme is used, a longitudinal communication range of 64.7 m can be achieved. With 8-PPM the communication distance can reach 85.1 m. In addition, the photocurrent induced by the daylight solely has already reached 271 mA, which is far beyond the PD's saturation limit of 6.67 mA. A great improvement has been achieved with the advanced receiver, as illustrated in Figure 6. When OOK is applied, a communication distance of 101.8 m can be achieved. With 8-PPM scheme a distance of 133.8 m is obtained. The application of the LC panel helps to solve the saturation problem effectively by controlling the pass region of the light. Therefore, the dynamic range of the advanced receiver is much broader compared to the cases when no spatial filtering is applied.

The second simulation is based on a multiuser scenario, where two equal headlights which are identically modulated are present in front of the receiver. One headlight functions as the transmitter and is put directly in front of the receiver at a longitudinal distance D . The other one is the interference source which is located next to the signal source with a distance Δx , as shown in Figure 2.

At three different longitudinal distances of 10, 25 and 50 m, the Signal-to-Interference Ratio (SIR) (cf. Equation (2)) of the receiver with respect to different lateral distances Δx is evaluated. The minimum Δx value is set to 0.5 m, which is the minimum safety distance for two vehicles to drive along.

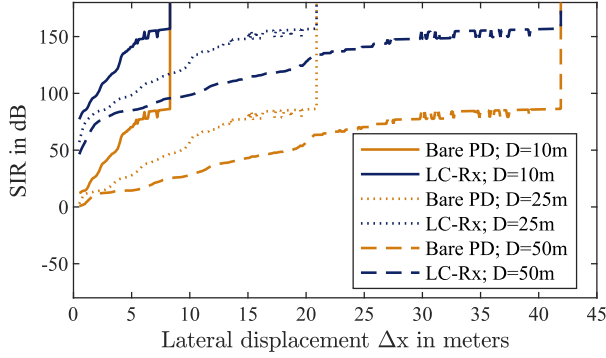


Fig. 7. SIR at the receiver at $D = 10, 25$ and 50 m

The expression of SIR is then given as

$$SIR = \frac{I_s^2}{I_i^2}, \quad (2)$$

where I_s and I_i are signal-induced photocurrent and interference-induced photocurrent at the PD, respectively. The SIR of the receiver at different longitudinal distances are shown in Figure 7.

It is shown in the figure that if only the PD is applied the SIR first increases with the lateral distance Δx , because the power of interference light drops considerably in this direction. Besides, with an increasing observing angle θ , the SIR decreases, since the illuminance of the interference light on the receiver is proportional to the cosine of this angle. After a certain distance, the receiver falls out of the interference source's FoV, and no interference is present at the receiver's surface. From this point on, the SIR remains infinite and is out of the discussion. When $D = 50$ m, at two typical lateral distances $\Delta x = 0.5$ m and $\Delta x = 3$ m, the SIR values are 0.70 dB and 12.62 dB, respectively.

When only optics is applied in front of the PD without any LC-panel, the performance of the receiver is expected to be improved, because with θ increasing, some peripheral light is vignetted and, thus, a lower interference intensity is received, and a higher SIR is obtained, which is a benefit in our scenario. However, the small FoV of the receiver due to the limited size of the PD limits the angular communication range and makes it hard to have a communication coverage for both neighboring lanes.

The double sides of the small FoV are well demonstrated in this assumption. Therefore, when we apply only front optics without a spatially filter element in front of a PD, a trade-off between the FoV and the communication distance has to be made. However, when the LC panel is added to the receiver, the performance exhibits an enormous improvement. With a very small θ , a large proportion of the signal light is blocked together with the interference light; however, as long as there is a clearance between two spots, the SIR can still reach a high level. At the first stage, the SIR increases fast with the lateral distance because the overlapped region

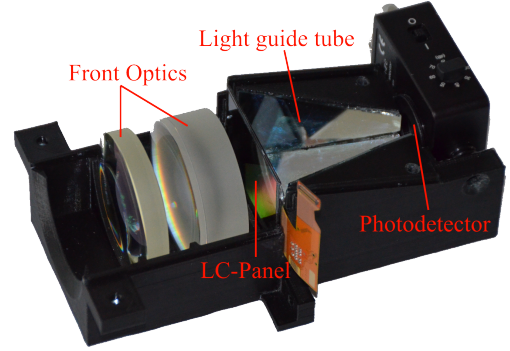


Fig. 8. The cross-sectional view of the prototype

is getting smaller and thus the signal light which can pass through the LC panel is increasing. At the second stage, the two spots are totally separated, the rising starts to slow down and has almost the same slope as the other two configurations since they are all subject to the cosine law of the illuminance. The SIR at this stage is mainly decided by the contrast ratio of the LC panel. With a higher contrast ratio, the SIR can be further improved. In order to have a quantitative comparison to the situation where only the PD is used, at $\Delta x = 0.5$ m and $\Delta x = 3$ m, the SIR values are increased to 46.33 dB and 79.76 dB, which proves the receiver's ability to ensure the communications even when a very strong and modulated interference source is placed nearby.

The cross-sectional view of the prototype can be seen in Figure 8. The size of the prototype is 90 mm \times 60 mm \times 145 mm, which makes it feasible for implantation in vehicles.

Practical measurements have been carried out with this prototype under an outdoor scenario in a very bright sunny day, with the illuminance of the daylight varied continuously between 90 klx and 120 klx. The headlights are not optically modified, only a small circuit board is implemented which can drive the LEDs at higher frequencies. The control of the LC panel is accomplished in a static way and 8 image patterns can be chosen from the storage. The headlights are driven by a 200 kHz sinus wave. Firstly, a single bare PD with a gain of 0 dB is used as the receiver.

When the headlight is 5 m away from the receiver, the signal peak occurs at 200 kHz can be easily distinguished from the electrical frequency spectrum, and a SNR of 15.1 dB is achieved. However, when the distance increases to 10 m, the signal can be hardly separated from the noises. Typically, by increasing the gain of the PD, SNR can be improved; however, with a higher gain the PD is always saturated under the aforementioned illuminance conditions. The empirical results attest that a single PD without further modifications is highly unqualified to serve as the receiver in V-VLC applications where dynamic scenarios can always emerge. Unlike the scenario in this measurement, a real traffic scenario can include more noise sources than just the daylight, which means the saturation problem of the PD is a serious challenge and thus the communication link can be easily lost.

Substituting the bare PD with our newly designed prototype,

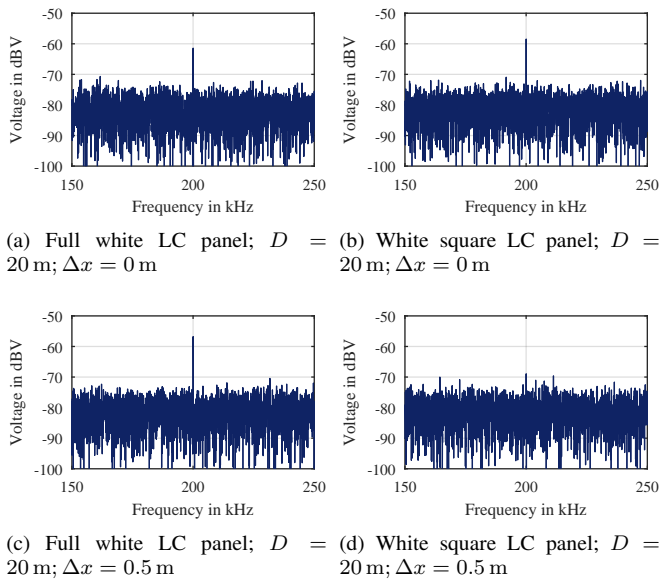


Fig. 9. Outdoor experiment with $D = 20$ m and $\Delta x = \{0 \text{ m}, 0.5 \text{ m}\}$.

the effective communication range is greatly extended. With a square pattern applied at the LC panel, the DC component decreases from -2.1 dBV to -12.5 dBV even with a higher gain of 30 dB which is chosen according to the illuminance of the day, addressing the severe saturation problem. At a longitudinal distance of 5 m, SNR rises to 28.4 dB. With the distance further increased to 10 m, unlike the situation with a single PD, a SNR of 17.3 dB can still be achieved. By comparing the results using full white pattern and square pattern on the LC panel, a considerable decrease in DC component and slight increase in SNR indicate that the shot noise induced by the background daylight only contributes to a small fraction of the total noises and that the thermal noises of the PD dominate, which affect the performance of the receiver stronger than expected. Nevertheless, the performance of the prototype in terms of SNR surpasses a conventional PD to a great extent.

Besides the improvement in SNR, another major achievement made by the prototype is its enhanced robustness to the interference caused by other artificial light sources. When several cars equipped with VLC transmitters are located within the reception angle of the receiver, if the modulation frequencies of the transmitters are similar, the presence of interference sources can have a great negative impact on the visible light communications [12]. During each measurement, the headlight is first measured as the transmitter and then moved outwards and measured as the interference source

TABLE II
SIR PERFORMANCE IN THE OUTDOOR EXPERIMENT

D (m)	Δx (m)	Receiver	SIR (dB)
5	0.5	PD	0.6
20	0.5	PD	no signal detected
5	0.5	LC-based receiver	11.4
20	0.5	LC-based receiver	12.1

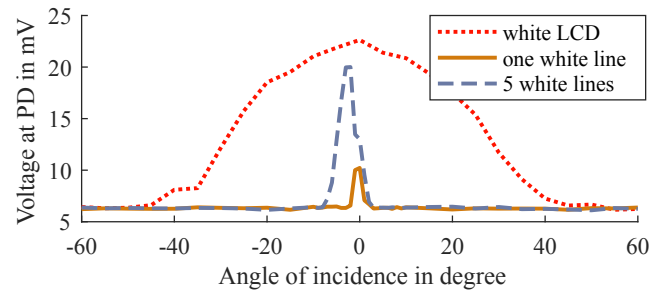


Fig. 10. Angular resolving capabilities of the LC based receiver with different patterns

with identical configuration as the transmitter. The results obtained from the measurements are presented in Table II. The frequency spectra of transmitter and interference source received by a single PD are nearly identical and the signal peaks occur at the same frequency, which means it would be impossible to separate the interference by electrical means, e.g., the electrical filter. Therefore, a very low SIR of only 0.6 dB is obtained. If the interference source is assumed as another V-VLC transmitter, additional multiple access schemes, for example in frequency, time or code domain, would be needed to enable communications. This would introduce fewer resources in terms of time and bandwidth for each user.

If the interference is assumed as another modulated light source, the presence of this light source would prevent a reliable communication. When the signal source and the interference source have similar optical spectra with peaks occurring within similar wavelength ranges, little interference light can be filtered out by an optical filter. The prototype is however intentionally designed to address this issue. When we replaced the PD by our prototype, a strong interference is shown in the frequency spectrum if a full white pattern is applied on the LC panel. But the interference can be effectively blocked out when a proper image pattern is chosen at the LC panel. The application of the square pattern in the center of the LC panel leads to an increased SIR at 5 m. The resolving ability does not degrade at a further distance of 20 m, with a stronger illuminance at the transmitting side, SIR again increased. The frequency spectra received with an oscilloscope can be seen in Figure 9. It is worth to notice that the average value of the noises in a certain frequency range are used in the calculation, but in practice the noise values fluctuate between -90 dBV and -120 dBV with the oscilloscope used in the measurements, which means values of SIR calculated from the spectra are largely constrained. Therefore, the SIR values presented here certify in a relative way that the LC-based receiver we have developed is highly promising in terms of interference blocking. The characterization on the angular resolving capability of our designed receiver is also measured and shown in Figure 10. The possibility to distinguish two modulated sources with angular difference about 1° shows the potentiality of this prototype to be applied under multiuser traffic scenarios.

VI. CONCLUSION

In this paper, we presented a receiver prototype that can reduce the negative impact of interference noises to a minimum by spatially filtering the received light. This could enable visible light communications even in the presence of strong interference noises and could enable light weight communication protocols. By filtering multiuser interference in a physical way, the latency could be decreased as well. In simulations the signal-to-noise ratio have been increased by blocking ambient light and the interference can be decreased to a minimum. In the outdoor measurements we have verified that the interference could be reduced by more than 12 dB. Overall, we see our system as a very relevant building block for future heterogeneous ITS supporting cooperative driving applications in tightly controlled real-time applications.

There are several aspects that can be further advanced. First, there are losses resulted by the imperfect light concentrator behind the LC panel due to back reflections and lossy multi-reflections. This can be addressed by a Compound-Parabolic-Concentrator (CPC). Second, the major losses due to the polarizers of the LC panel can be decreased by applying a polarization conversion system in front of the LC panel. A future alternative to the LC panel with similar functions but a higher transmittance could be electrostatic microshutter arrays which have been applied for the James Webb Space Telescope developed by NASA [25]. The programmable arrays can open and close each small window by electrostatic forces. But the problems such as individual controlling, fatigue and operating temperature range need to be settled before the implementation, also the high costs in next years could be expected and will be an obstacle towards commercialization. Therefore, LC panels can still dominate and play an irreplaceable role in the spatial-filtering-based receivers in the next years.

REFERENCES

- [1] P. Papadimitratos, A. L. Fortelle, K. Evenssen, R. Brignolo, and S. Cosenza, "Vehicular communication systems: Enabling technologies, applications, and future outlook on intelligent transportation," *IEEE communications magazine*, vol. 47, no. 11, pp. 84–95, Nov. 2009.
- [2] ETSI, "Intelligent Transport Systems (ITS); Vehicular Communications; Basic Set of Applications; Part 2: Specification of Cooperative Awareness Basic Service," ETSI, EN 302 637-2 V1.3.2, Nov. 2014.
- [3] IEEE, "IEEE Standard for Wireless Access in Vehicular Environments (WAVE) - Networking Services," IEEE, Std 1609.3-2010, Dec. 2010.
- [4] M. Gonzalez-Martín, M. Sepulcre, R. Molina-Masegosa, and J. Gozalvez, "Analytical Models of the Performance of C-V2X Mode 4 Vehicular Communications," *IEEE Transactions on Vehicular Technology*, vol. 68, no. 2, pp. 1155–1166, Feb. 2019.
- [5] C. Sommer and F. Dressler, *Vehicular Networking*. Cambridge University Press, Nov. 2014.
- [6] S.-H. Yu, O. Shih, H.-M. Tsai, N. Wisitpongphan, and R. Roberts, "Smart automotive lighting for vehicle safety," *IEEE Communications Magazine*, vol. 51, no. 12, pp. 50–59, Dec. 2013.
- [7] M. Abualhoul, M. Marouf, O. Shagdar, and N. Fawzi, "Platooning Control Using Visible Light Communications: A Feasibility Study," in *IEEE Intelligent Transportation Systems Conference (ITSC 2013)*, The Hague, The Netherlands: IEEE, Oct. 2013.
- [8] B. Béchadargue, L. Chassagne, and H. Guan, "Suitability of visible light communication for platooning applications: An experimental study," in *IEEE Global LIFI Congress (GLC 2018)*, Paris, France: IEEE, Feb. 2018.
- [9] A. Memedi, C. Tebruegge, J. Jahneke, and F. Dressler, "Impact of Vehicle Type and Headlight Characteristics on Vehicular VLC Performance," in *10th IEEE Vehicular Networking Conference (VNC 2018)*, Taipei, Taiwan: IEEE, Dec. 2018.
- [10] S. Ishihara, R. V. Rabsatt, and M. Gerla, "Improving Reliability of Platooning Control Messages Using Radio and Visible Light Hybrid Communication," in *7th IEEE Vehicular Networking Conference (VNC 2015)*, Kyoto, Japan: IEEE, Dec. 2015, pp. 96–103.
- [11] M. Schettler, A. Memedi, and F. Dressler, "Deeply Integrating Visible Light and Radio Communication for Ultra-High Reliable Platooning," in *15th IEEE/IFIP Conference on Wireless On demand Network Systems and Services (WONS 2019)*, Wengen, Switzerland: IEEE, Jan. 2019.
- [12] W.-H. Shen and H.-M. Tsai, "Testing Vehicle-to-Vehicle Visible Light Communications in Real-World Driving Scenarios," in *9th IEEE Vehicular Networking Conference (VNC 2017)*, Torino, Italy: IEEE, Nov. 2017, pp. 187–194.
- [13] A.-M. Cailean and M. Dimian, "Current Challenges for Visible Light Communications Usage in Real-World Applications: A Survey," *IEEE Communications Surveys & Tutorials*, no. 99, May 2017.
- [14] P. H. Pathak, X. Feng, P. Hu, and P. Mohapatra, "Visible Light Communication, Networking, and Sensing: A Survey, Potential and Challenges," *IEEE Communications Surveys & Tutorials*, vol. 17, no. 4, pp. 2047–2077, Sep. 2015.
- [15] Y. Goto, I. Takai, T. Yamazato, H. Okada, T. Fujii, S. Kawahito, S. Arai, T. Yendo, and K. Kamakura, "A New Automotive VLC System Using Optical Communication Image Sensor," *IEEE Photonics Journal*, vol. 8, no. 3, pp. 1–17, Jun. 2016.
- [16] X. Huang, S. Chen, Z. Wang, J. Shi, Y. Wang, J. Xiao, and N. Chi, "2.0-Gb/s Visible Light Link Based on Adaptive Bit Allocation OFDM of a Single Phosphorescent White LED," *IEEE Photonics Journal*, vol. 7, no. 5, pp. 1–8, Oct. 2015.
- [17] M. S. Amjad, C. Tebruegge, A. Memedi, S. Kruse, C. Kress, C. Scheytt, and F. Dressler, "An IEEE 802.11 Compliant SDR-based System for Vehicular Visible Light Communications," in *IEEE International Conference on Communications (ICC 2019)*, Shanghai, China: IEEE, May 2019.
- [18] J. B. Carruther and J. M. Kahn, "Angle diversity for nondirected wireless infrared communication," *IEEE Transactions on Communications*, vol. 48, no. 6, pp. 960–969, Jun. 2000.
- [19] M. A. El-Shimy and S. Hranilovic, "Spatial-Diversity Imaging Receivers for Non-Line-of-Sight Solar-Blind UV Communications," *Journal of Lightwave Technology*, vol. 33, no. 11, pp. 2246–2255, Jun. 2015.
- [20] Z. Chen, D. A. Basnayaka, X. Wu, and H. Haas, "Interference Mitigation for Indoor Optical Attocell Networks Using an Angle Diversity Receiver," *Journal of Lightwave Technology*, vol. 36, no. 18, pp. 3866–3881, Sep. 2018.
- [21] W.-H. Shen, P. W. Chen, and H.-M. Tsai, "Vehicular Visible Light Communication with Dynamic Vision Sensor: A Preliminary Study," in *10th IEEE Vehicular Networking Conference (VNC 2018)*, Taipei: IEEE, Dec. 2018.
- [22] J. Kratochvil, "Exterior lighting used for C2C communication – High Speed & High Resolution Smart Detector," in *12th International Symposium on Automotive Lighting (ISAL 2017)*, Darmstadt, Germany, Sep. 2017, pp. 575–578.
- [23] C. B. Martin, "Design issues of a hyperfield fisheye lens," in *Novel Optical Systems Design and Optimization*, vol. 5524, Denver, CO: SPIE, Oct. 2004.
- [24] N. Lourenco, D. Terra, N. Kumar, L. N. Alves, and R. L. Aguiar, "Visible Light Communication System for outdoor applications," in *8th International Symposium on Communication Systems, Networks & Digital Signal Processing (CSNDSP 2012)*, Poznan, Poland: IEEE, Jul. 2012.
- [25] M. J. Li, A. D. Brown, D. E. Burns, D. P. Kelly, K. Kim, A. S. Kuttyrev, S. R. McCandliss, S. H. Moseley, V. Mikula, and L. H. Oh, "Electrostatic microshutter arrays," in *19th International Conference on Solid-State Sensors, Actuators and Microsystems (TRANSDUCERS 2017)*, Kaohsiung, Taiwan: IEEE, Jun. 2017, pp. 2235–2238.